# Failure of microtubule-mediated peroxisome division and trafficking in disorders with reduced peroxisome abundance

**Tam Nguyen[1,2], Jonas Bjorkman[1,2], Barbara C. Paton[3,4] and Denis I. Crane[1,2,*]**

[1]Cell Biology Group, Eskitis Institute for Cell and Molecular Therapies, and [2]School of Biomolecular and Biomedical Science, Griffith University, 170 Kessels Road, Nathan, Brisbane, Queensland 4111, Australia
[3]Department of Genetic Medicine, Women's and Children's Hospital, 72 King William Road, North Adelaide, South Australia, 5006, Australia
[4]Department of Pediatrics, University of Adelaide, Adelaide, South Australia, 5005, Australia
*Author for correspondence (e-mail: d.crane@griffith.edu.au)

## Summary

In contrast to peroxisomes in normal cells, remnant peroxisomes in cultured skin fibroblasts from a subset of the clinically severe peroxisomal disorders that includes the biogenesis disorder Zellweger syndrome and the single-enzyme defect D-bifunctional protein (D-BP) deficiency, are enlarged and significantly less abundant. We tested whether these features could be related to the known role of microtubules in peroxisome trafficking in mammalian cells. We found that remnant peroxisomes in fibroblasts from patients with PEX1-null Zellweger syndrome or D-BP deficiency exhibited clustering and loss of alignment along peripheral microtubules. Similar effects were observed for both cultured embryonic fibroblasts and brain neurons from a PEX13-null mouse with a Zellweger-syndrome-like phenotype, and a less-pronounced effect was observed for fibroblasts from an infantile Refsum patient who was homozygous for a milder *PEX1* mutation. By contrast, such changes were not seen for patients with peroxisomal disorders characterized by normal peroxisome abundance and size. Stable overexpression of PEX11β to induce peroxisome proliferation largely re-established the alignment of peroxisomal structures along peripheral microtubules in both PEX1-null and D-BP-deficient cells. In D-BP-deficient cells, peroxisome division was apparently driven to completion, as induced peroxisomal structures were similar to the spherical parental structures. By contrast, in PEX1-null cells the majority of induced peroxisomal structures were elongated and tubular. These structures were apparently blocked at the division step, despite having recruited DLP1, a protein necessary for peroxisome fission. These findings indicate that the increased size, reduced abundance, and disturbed cytoplasmic distribution of peroxisomal structures in PEX1-null and D-BP-deficient cells reflect defects at different stages in peroxisome proliferation and division, processes that require association of these structures with, and dispersal along, microtubules.

Key words: Peroxisome biogenesis, Peroxisomal disorders, Organelle division, Microtubule trafficking, PEX11β

## Introduction

The peroxisome is an organelle that makes an essential contribution to cellular metabolism (van den Bosch et al., 1992). In humans, the essential nature of the peroxisome is underscored by a group of genetic disorders involving peroxisomal metabolic dysfunction and widespread organ pathology (Moser, 1993; Schutgens et al., 1986). Peroxisomal disorders have been classified into two main categories: the peroxisome biogenesis disorders (PBDs), represented by the severe Zellweger syndrome (ZS), in which the peroxisome lacks most or multiple content proteins and sometimes membrane, and single-enzyme disorders, in which there is loss of a specific component of a peroxisomal metabolic pathway (Gould et al., 2001; Moser, 1993; Moser, 1996; Wanders et al., 1995). Whereas the genetic basis of most peroxisomal disorders is now known (Gould and Valle, 2000; Wanders and Waterham, 2005; Weller et al., 2003), the molecular pathogenesis of the multi-system abnormalities in these disorders, including the severe neurodegeneration, is still unresolved.

A proposed alternative means of differentiating peroxisomal disorders that crosses the traditional clinical, genetic and biochemical criteria is based on peroxisome abundance and morphology (Chang et al., 1999). Disorders of low peroxisome abundance include ZS and two single-enzyme disorders, acyl-CoA oxidase deficiency and D-bifunctional protein (D-BP; or multifunctional enzyme/protein 2, MFE2/MFP2) deficiency. The 'peroxisome abundance' classification also seemingly accounts for the morphological differences of peroxisomes in the different disorders: in ZS, remnant peroxisomes are present as 'membrane ghosts', enlarged vesicles lacking content proteins (Santos et al., 1988); in both D-BP deficiency and acyl-CoA oxidase deficiency, peroxisomes are also enlarged, for reasons that are not understood, and comparable in size to ZS ghosts (Hughes et al., 1990; Poll-The et al., 1988; Suzuki et al., 1994; van Grunsven et al., 1999). By contrast, peroxisomes are of normal abundance and morphology in other single-enzyme or single-protein deficiencies such as X-linked adrenoleukodystrophy (X-ALD), and in rhizomelic

chondrodysplasia punctata (RCDP), the latter representing the non-Zellweger syndrome class of biogenesis disorders characterized by loss of PTS2 import (Purdue et al., 1999; Purdue et al., 1997; Smith et al., 1999). Intriguingly, Gould and colleagues (Chang et al., 1999; Li and Gould, 2002; Schrader et al., 1998) demonstrated that the reduced peroxisome abundance of ZS cells could be restored by overexpression of the peroxisomal membrane protein PEX11β, a peroxin implicated in peroxisome proliferation and division (Schrader et al., 1998). These findings indicate that remnant peroxisomes are competent for PEX11β-mediated proliferation and division, and that this process does not require peroxisomal metabolic activity (Li and Gould, 2002).

In the context of these findings, the phenotype of the PEX11β-null mouse is of particular relevance. Peroxisomes, with an apparent complement of content proteins, are present in PEX11β-null cells (Li et al., 2002b). Surprisingly, however, these mice show the clinical hallmarks of the severe ZS phenotype, but little loss of the 'signature' peroxisomal metabolic pathways of VLCFA β-oxidation and ether lipid (plasmalogen) synthesis (Li et al., 2002b). In exploring an alternative explanation for the molecular pathogenesis of PEX11β-null mice, it is of interest that two significant changes accompanied the loss of cellular PEX11β, namely reduced peroxisome abundance and increased peroxisome clustering. Taken together, these findings point to an alternative model of pathogenesis in which disease phenotype correlates with abnormalities in peroxisome abundance and/or distribution in cells.

One cellular process that may provide a unifying theme for these findings is microtubule-based peroxisome morphogenesis and movement. Previous studies have established that peroxisomes associate with microtubules, and that microtubule-mediated peroxisome motility is the primary mode of regulation of peroxisome morphology and trafficking in cells (Rapp et al., 1996; Schrader, 2001; Schrader et al., 1996; Schrader et al., 2000; Thiemann et al., 2000; Wiemer et al., 1997). Also, in the context of disease pathogenesis, it is now acknowledged that mutations affecting proteins involved in intracellular trafficking via the cytoskeleton underlie many neurodegenerative diseases (Aridor and Hannan, 2000).

In this research, we have tested the hypothesis that microtubule-mediated peroxisome trafficking is perturbed in cells with reduced abundance and altered cytoplasmic distribution of remnant peroxisomes. We demonstrate a striking change to the cytoplasmic distribution of peroxisomal structures in such cells, and show that the abundance, cytoplasmic distribution and alignment along microtubules of these structures can be restored by overexpression of PEX11β. We interpret this result to indicate that peroxisome proliferation, division and trafficking along microtubules are mechanistically-related processes that occur independently of peroxisomal metabolic activity.

## Results

### Peroxisomes are distributed along microtubules in normal human and mouse fibroblasts

It has been demonstrated that peroxisomes associate with microtubules in certain mammalian cell types (Schrader, 2001; Schrader et al., 1996; Schrader et al., 2000; Schrader et al., 2003; Wiemer et al., 1997), but such an association has not been well established for mouse or human fibroblasts. To detect peroxisomal membranes in both normal cells and those with abnormalities in peroxisome matrix content and morphology, we prepared a rabbit antibody to the murine peroxisomal membrane protein PEX14. The generated antibody recognized a protein of approximately 57 kDa molecular mass, which is in accord with that reported for the human and CHO cell PEX14 proteins (Fransen et al., 1998; Shimizu et al., 1999). As expected, the identified protein behaved as an organelle protein upon analysis of liver fractions from a wild-type mouse, in that it was distributed in a similar way to both the peroxisomal membrane protein PEX13 and the matrix protein catalase (Fig. 1A, left panel). In liver fractions from PEX13-null mice, in which peroxisomal matrix protein import is defective, PEX14 was still present, albeit at slightly lower levels, and shifted from the organelle pellet fraction to the post-organellar supernatant containing unimported catalase (Maxwell et al., 2003) (Fig. 1A, right panel). This latter result is consistent with the presence of remnant peroxisomes (peroxisomal ghosts) with lower density and thus reduced capacity to be pelleted by centrifugation. To validate the use of PEX14 as a marker in cell studies, we carried out immunofluorescence analysis of wild-type mouse embryonic fibroblasts (MEFs; not shown) and normal human skin fibroblasts (HSFs; Fig. 1B) expressing EGFP protein fused to the consensus peroxisome targeting signal type 1 (PTS1). In both cell types, the PEX14 antibody decorated cytoplasmic organelles that had imported EGFP, confirming the specificity of this antibody in recognizing peroxisomal structures in both mouse and human cells.

To determine the distribution of peroxisomes relative to the
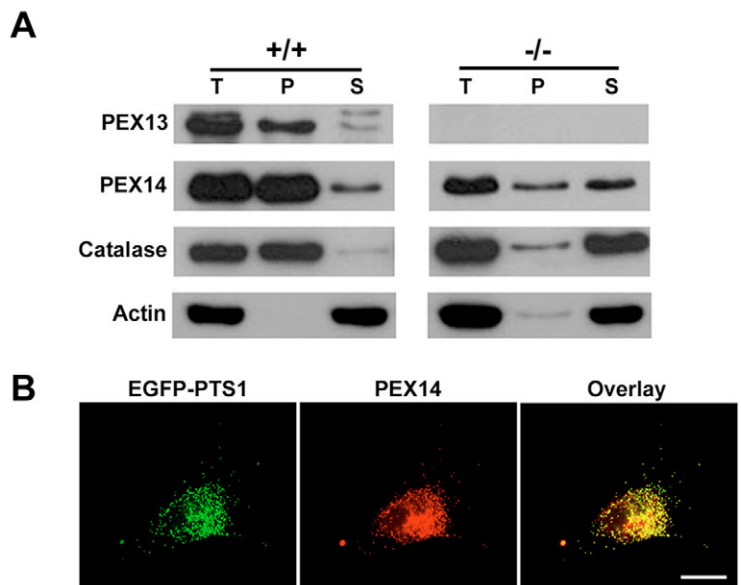


**Fig. 1.** PEX14 localizes peroxisomal structures in mammalian cells. (A) Western blot analysis of mouse liver fractions. T, total liver homogenate; P, organelle pellet; S, Post-organellar supernatant. +/+, wild-type mice; –/–, PEX13-null mice. (B) Immunofluorescence microscopy of a normal human skin fibroblast transfected with plasmid expressing EGFP-PTS1 fusion protein. Green, EGFP; red, PEX14. Bar, 20 μm.

microtubule network in cultured normal control HSFs and wild-type MEFs, we carried out fluorescence microscopy using the PEX14 antibody in combination with an α-tubulin

subunit antibody to decorate microtubules (Fig. 2A). In both HSFs and MEFs, peroxisomes were abundant and distributed throughout the cytoplasm. The use of confocal laser-scanning microscopy (CLSM) to examine the proximity of peroxisomes to peripheral microtubules revealed that most peroxisomes aligned adjacent to and along individual microtubules. This result concurs with findings on other mammalian cells (Rapp et al., 1996; Schrader, 2001; Schrader et al., 1996; Schrader et al., 2000; Thiemann et al., 2000; Wiemer et al., 1997).

### Microtubule cytoskeleton-perturbing drugs disrupt the spatial organization of peroxisomes in cultured fibroblasts

To establish whether microtubules are essential for normal peroxisome distribution in fibroblasts, we used nocodazole, a microtubule-depolymerising drug, to disperse the microtubule network. Treatment of normal HSF cells with 20 μM nocodazole for 20 hours led to microtubule depolymerization, as evident by the diffuse cytoplasmic staining with tubulin antibody (Fig. 2B, top). Peroxisomes in these cells clustered at several locations, including at the cytoplasmic face of the nuclear envelope. A more extreme clustering of peroxisomes near the cell surface was observed for normal MEFs similarly treated (Fig. 2B, bottom). We assessed the generality of the disruptive effect of nocodazole by also observing effects on mitochondria, another organelle whose motility requires microtubules (Welte, 2004). Mitochondria in untreated cultured HSFs, stained using MitoTracker Green FM dye, were dispersed as an intricate reticulum throughout the cell cytoplasm (Fig. 2C, top). In HSFs treated with nocadozole, mitochondrial distribution was severely disrupted and characterized by clustering near the nucleus, including some distinct perinuclear clustering as seen for peroxisomes (Fig. 2C, bottom). The effect was similar in wild-type MEFs (not shown). As predicted, these results demonstrate that perturbation of the microtubule network leads to aberrant peroxisome (and mitochondrial) distribution, including clustering. The inference from these findings is that the normal cellular distribution of peroxisomes is dependent on motility via the microtubule network.
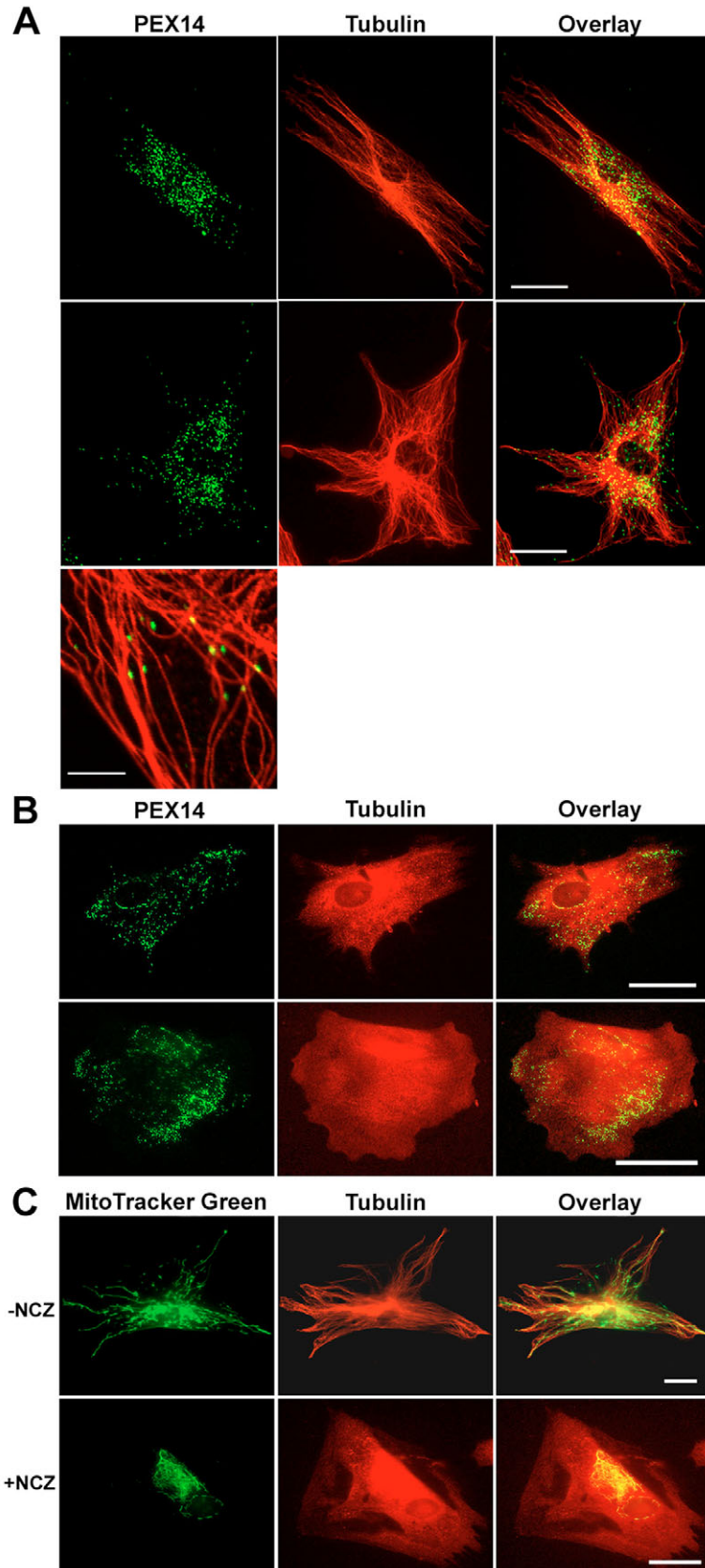


**Fig. 2.** Peroxisomes align with, and are dispersed along, microtubules in cultured fibroblasts.
(A) Immunofluorescence microscopy of peroxisomes and microtubules in control HSFs (top) and wild-type MEFs (middle). Bottom panels show confocal laser-scanning microscopy of a HSF. Green, PEX14; red, α-tubulin.
(B) HSFs (top panels) and wild-type MEFs (bottom panels) treated with 20 μM nocodazole for 20 hours. PEX14 (green); α-tubulin (red). (C) Mitochondria (green) and microtubules (red) detected using MitoTracker Green FM dye and α-tubulin antibody, respectively, in untreated (–NCZ, top panels) and nocodazole treated (+NCZ, bottom panels) HSFs. Bars, 20 μm (top and middle panel in A; and B and C); 5 μm (bottom panel in A).

## The distribution and microtubule association of remnant peroxisomes is perturbed in cell lines featuring both defective peroxisome biogenesis and reduced peroxisome abundance

To address our primary hypothesis that reduced peroxisome abundance and altered morphology correlate with perturbed microtubule-based peroxisomal distribution, we carried out immunofluorescence microscopy of HSFs from patients representing a range of peroxisomal disorders, as well as of MEFs from the PEX13-null mouse with a ZS-like phenotype.

In cells from a PEX1-null ZS patient (patient 4065), in which there is loss of both PTS1 and PTS2 peroxisomal import (Maxwell et al., 2002; Maxwell et al., 1999), the microtubule network appeared normal, but the abundance of (remnant) peroxisomes was reduced to ~20% of the normal level ($87\pm14$ vs $421\pm31$ peroxisomes/cell for normal control cells; mean $\pm$ s.e.m., $n=5$ cells/experiment), whereas the size of these structures was increased (cross-sectional area of $14.0\pm1.1$ pixels vs $9.8\pm1.5$ pixels for normal controls; $n=5$) (Fig. 3A). These latter observations are in accord with results from previous studies and reflect the formation of fewer, enlarged peroxisomal vesicular 'ghosts' (Chang et al., 1999; Santos et al., 1988). Of particular interest, however, was the spectacular change in the distribution of these remnant peroxisomes in PEX1-null cells, characterized by varying degrees of clustering and altered distribution. Cells fell into three roughly equally represented groups (Fig. 3A): the first group (top) showed slight retraction of peroxisomal structures towards the cell center and minor clustering; the second group (middle) showed more pronounced perinuclear segregation of peroxisomal structures, again with minor clustering; the third group (bottom) showed striking clustering of most peroxisomal structures at different locations in different cells, but never at the microtubule organizing centre (MTOC, see arrow). Although we predicted that the peroxisomal structures in these cells might no longer associate with microtubules, CSLM showed instead that most, but not all, of these structures were still aligned along microtubules (Fig. 3B).

As additional controls, we demonstrated that the peroxisomal structures in PEX1-null cells did not colocalize with LysoTracker dye (Fig. 3C), thereby discounting a potential accumulation in lysosomes as part of an autophagic process. We also tested for possible changes to the distribution of mitochondria in these cells using MitoTracker dyes. The mitochondrial network (Fig. 3D) was not significantly altered when compared with those in normal control cells. A similar result was shown for PEX13-null MEFs (not shown). Moreover, there was apparent absolute fluorescence colocalization in these cells of MitoTracker Red CM-H$_2$XRos dye (representative of actively respiring mitochondria) and MitoTracker Green FM dye (a measure of mitochondrial abundance) (Fig. 3D), a finding that is consistent with normal metabolic activity of the majority of mitochondria in these cells. Thus, the organelle-trafficking defect observed for peroxisomes does not extend to mitochondria, nor, we assume, other organelles.
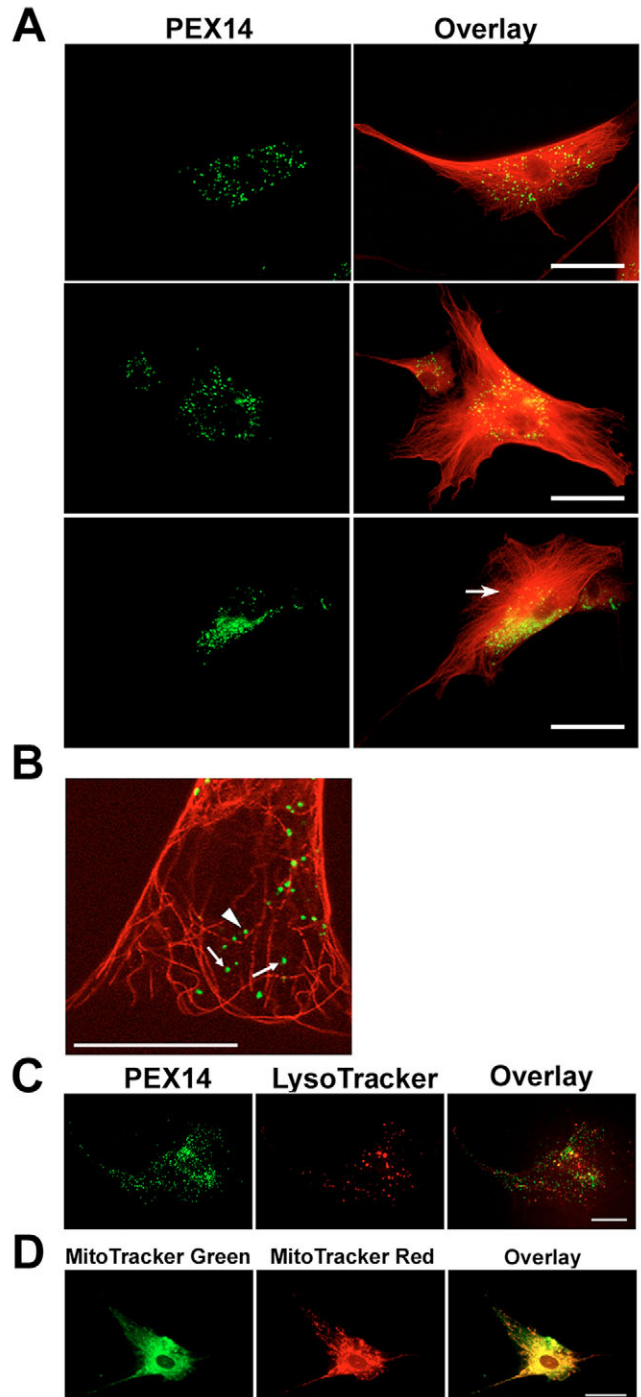


**Fig. 3.** Peroxisome abundance and distribution along peripheral microtubules are perturbed in PEX1-null ZS cells. (A) PEX1-null patient HSFs processed with antibodies against PEX14 (green) and α-tubulin (red). Top panels, minimal retraction of remnant peroxisomes; middle panels, pronounced remnant peroxisome retraction, with initial signs of clustering; bottom panels, dramatic clustering of remnant peroxisomes. Arrow indicates MTOC, corresponding to microtubule nucleation/anchor region. (B) Confocal laser-scanning microscopy showing remnant peroxisomes aligning (white arrowhead) or not aligning (white arrows) with microtubules. (C) PEX1-null cells stained for remnant peroxisomes using PEX14 antibody (green), and for lysosomes using LysoTracker Red DND-99 (red). (D) PEX1-null HSF cells stained for mitochondria using MitoTracker Green FM and MitoTracker Red CM-H$_2$XRos dyes. Bars, 20 μm (A,C,D); 5 μm (B).

In cells from an IRD patient (1772), corresponding to a milder PEX1 mutation in which PEX1 function is attenuated but not abolished (Maxwell et al., 2002), the abundance of remnant peroxisomes was also reduced ($102\pm15$ vs $421\pm31$ peroxisomes/cell, $n=5$), but the size of these structures was not significantly increased ($11.2\pm1.3$ pixels vs $9.8\pm1.5$ pixels). The association of remnant peroxisomes with the microtubule network was also perturbed, but at a level intermediate between that seen in normal controls and PEX1-null cells, with some of these structures still aligned along peripheral microtubules (Fig. 4A). Thus, this phenotype is consistent with the less severe PEX1 mutation being reflected in a less severe disturbance of microtubule-mediated peroxisome dispersal.

We also tested cells from an RCDP patient with PEX7 deficiency, a mutation leading to a specific defect in PTS2-dependent peroxisomal import – this disorder differs from ZS where both PTS1- and PTS2-dependent import are impaired. Both abundance ($432\pm34$ vs $421\pm31$ peroxisomes/cell, $n=5$) and size ($7.8\pm0.4$ pixels vs $9.8\pm1.5$ pixels) of remnant peroxisomes were normal in the PEX7-deficient cells. In addition, the peroxisomal structures were distributed uniformly throughout these cells, including at the microtubule plus ends near the cell surface (Fig. 4B).

The situation with the PEX13-null MEFs was similar to that for the PEX1-null (4065) HSFs. Remnant peroxisomes were readily detected using the PEX14 antibody, confirming that PEX14 is recruited to peroxisomal membranes in the absence of PEX13. These remnant structures were mostly located near the cell centre, displayed some minor clustering (Fig. 5A), reduced abundance ($104\pm21$ vs $284\pm43$ peroxisomes/cell for normal control cells; mean ± s.e.m., $n=5$) and significantly increased size ($15.2\pm1.3$ vs $8.0\pm0.3$ pixels for normal controls; $n=5$). As abnormal neuronal migration and neurodegeneration are hallmarks of severe peroxisomal disorders, and a feature of the PEX13-null mouse (Maxwell et al., 2003), we also tested whether the distribution of remnant peroxisomes was perturbed in cultured brain neurons from these mice. We found that whereas in PEX13 heterozygous neurons peroxisomes were abundant and distributed throughout the cell soma and along cell processes, in PEX13-null neurons, the remnant peroxisomes were clustered and restricted to the cell soma (Fig. 5B), similar to the effect observed for PEX13-null MEFs. Astrocytes in these cultures showed the same somal concentration of remnant peroxisomes (not shown).

Thus, the loss of distribution of remnant peroxisomes along microtubules, and specifically peripheral microtubules, only occurs in cells with a peroxisome biogenesis defect where the defect also leads to significantly reduced peroxisome abundance.

## Distribution and microtubule association of remnant peroxisomes is also perturbed in single-enzyme disorders with reduced peroxisome abundance

To determine whether perturbations in peroxisomal distribution and microtubule association were also characteristic of cells from patients with a single-enzyme defect in which there is also a concomitant reduction in peroxisome abundance, we
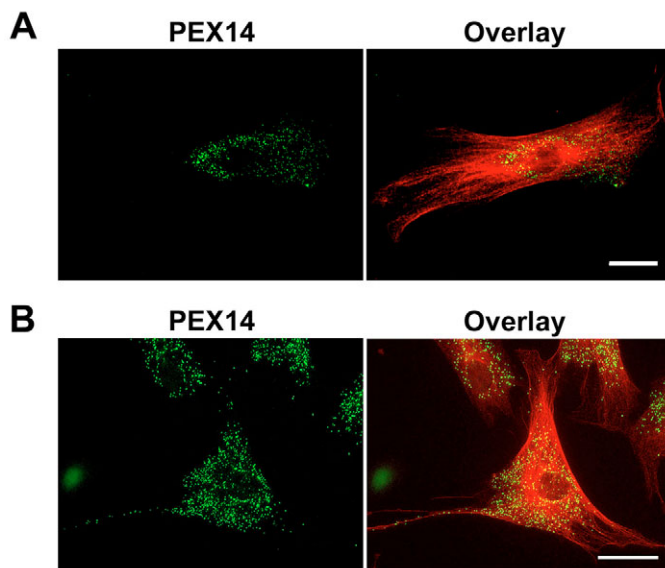


**Fig. 4.** Peroxisome abundance and distribution along peripheral microtubules are perturbed in fibroblasts from patients with IRD but not RCDP. Abundance and distribution of remnant peroxisomes along microtubules of cultured patient HSFs from patients with IRD (A) and RCDP (B), assessed by immunofluorescence using PEX14 (green) and α-tubulin (red) antibodies. Bars, 20 μm.
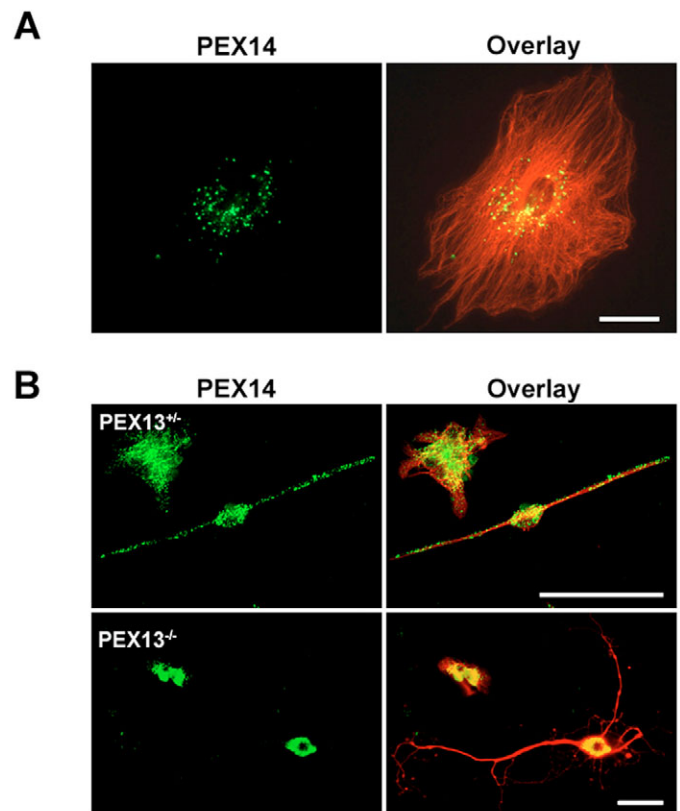


**Fig. 5.** Cultured MEFs and neurons from PEX13-null mice exhibit decreased remnant peroxisome abundance and distribution along peripheral microtubules. (A) PEX13-null MEFs and (B) PEX13 heterozygote (top panel) and PEX13-null (bottom panel) neurons (elongated cells in each case), assessed by immunofluorescence using PEX14 (green) and α-tubulin (red) antibodies. Bars, 20 μm.

# A
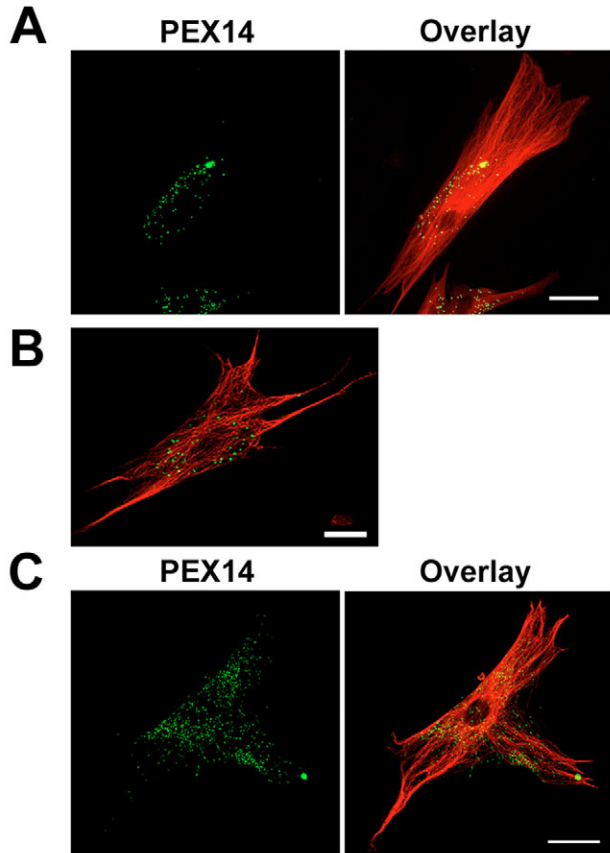


**Fig. 6.** The single-enzyme disorder, D-BP deficiency, is also characterized by decreased cellular peroxisome abundance and distribution along peripheral microtubules. (A) Peroxisome abundance and distribution along microtubules in HSFs from a D-BP-deficient patient. (B) Confocal laser-scanning microscopic image of a D-BP-deficient cell showing alignment of residual peroxisomes with microtubules. (C) Abundance and distribution of peroxisomes along microtubules in HSFs from an X-ALD patient. PEX14, green; $\alpha$-tubulin, red. Bars, 20 $\mu$m.

assessed HSFs from a D-BP deficient patient. The microtubule network in D-BP deficient HSFs appeared normal. However peroxisomes in these cells were larger (16.0±8.5 vs 9.8±1.5 pixels) and less abundant (71±27 vs 421±31) than in normal cells and showed the perturbation of peroxisomal distribution and microtubule alignment typical of PEX1-null Zellweger syndrome HSFs (Fig. 6A). CLSM demonstrated that most residual peroxisomes in these cells still aligned with microtubules (Fig. 6B). For comparison, we also analyzed cells from an X-ALD patient, as peroxisome abundance has previously been shown to be normal for such patients (Chang et al., 1999). We found that cells from this patient showed near-normal peroxisomal abundance (272±24 vs 421±31 peroxisomes/cell), normal peroxisome size (11.8±1.1 vs 9.8±1.5 pixels) and, of particular relevance here, normal cytoplasmic distribution and alignment of these peroxisomes along microtubules (Fig. 6B).

Taken together, the results indicate that a significant reduction in peroxisome abundance (down to ~20% of the normal level), correlates, in all cases, with loss of distribution of remnant peroxisomes along peripheral microtubules.

## Expression of PEX11β in PEX1-null and D-BP-deficient cells induces proliferation and distribution of different types of peroxisomal structures along peripheral microtubules

The previously reported effect of PEX11β in increasing the abundance of peroxisome ghosts (Chang et al., 1999; Li and Gould, 2002; Schrader et al., 1998) implied that this effect may have also restored the distribution of these structures along microtubules. To test this, we generated PEX1-null and D-BP-deficient cells stably overexpressing a C-terminal myc-epitope-tagged version of human PEX11β (PEX11βmyc). We observed that PEX11βmyc overexpression led to increased abundance of peroxisomal structures in PEX1-null (>fivefold) and D-BP deficient (>threefold) cells, and to a more uniform cellular distribution of these structures in both cases (PEX1-null cells: Fig. 7A; D-BP deficient cells: Fig. 7D). We did not see such effects in cells stably transfected with vector alone (not shown). Importantly, CLSM confirmed that PEX11βmyc-decorated peroxisomal structures were aligned along peripheral microtubules in PEX1-null cells (Fig. 7C) and D-BP deficient cells (Fig. 7F). However, the morphology of the induced peroxisomal structures was different in the two cell types. In D-BP-deficient cells they were spherical in shape, similar to those in mock-transfected and untransfected D-BP deficient cells (Fig. 7E). By contrast, many of the PEX11βmyc-decorated structures in PEX1-null cells had an elongated, tubular morphology (Fig. 7B) and exhibited alternating bands of PEX11βmyc immunostaining, similar to those previously identified following the very early periods of PEX11β activity (Schrader et al., 1998). We interpret these findings to indicate that in response to PEX11β overexpression, peroxisomes in D-BP deficient cells are competent for proliferation and division to daughter organelles, whereas remnant peroxisomes in PEX1-null cells are competent for proliferation but are blocked, at least partially, at the division step.

## DLP1 recruitment to induced peroxisomes

A recently reported function of PEX11β is to recruit the dynamin-like protein DLP1 to the peroxisomal membrane, at sites where PEX11β itself is sequestered away from other peroxisomal membrane proteins. It has been suggested that the role of DLP1 at this site may be to act as a 'pinchase' to release the daughter organelle (Koch et al., 2003; Li and Gould, 2003; Schrader et al., 1998). In view of this potentially central role of DLP1, we tested for DLP1 association with remnant peroxisomal membranes in D-BP deficient cells and PEX1-null cells using CLSM. In untransfected cells, DLP1 was essentially segregated from peroxisomal structures in both cases (Fig. 8A). In D-BP-deficient cells overexpressing PEX11βmyc, DLP1 was detected on a sub-population of peroxisomal structures. DLP1 was more abundant on the PEX11βmyc-decorated tubular structures generated in PEX1-null cells (Fig. 8B). For D-BP deficient cells, we interpret these findings to indicate that the overall process of peroxisomal proliferation and division has occurred effectively under the influence of PEX11βmyc, but that DLP1 is still associated with some peroxisomes owing to the ongoing PEX11βmyc activity. By contrast, for PEX1-null cells, we speculate that PEX11βmyc-dependent recruitment of DLP1 to elongating peroxisomal structures is occurring, but this alone has not been sufficient to drive these

peroxisomal structures through the division step, thus explaining the significantly greater retention of DLP1 at these membranes.

## Discussion

Reduced (remnant) peroxisome abundance is a feature common to a number of peroxisomal disorders (Chang et al., 1999). Disorders with this phenotype do not belong to any one genetic or disorder sub-group, but comprise those at the severe end of the Zellweger spectrum, along with the two single-enzyme disorders D-BP deficiency and acyl-CoA oxidase deficiency (Chang et al., 1999). Reduced peroxisome abundance of this order is not a feature of the remaining peroxisomal disorders, which include the non-Zellweger

biogenesis disorder RCDP, and other single-enzyme or single-protein disorders such as X-ALD. Our findings here concur with these previously reported relationships, but extend this link to include an effect on the distribution of peroxisomes along the microtubule network. Specifically, our data indicate that reduced abundance of remnant peroxisomes correlates with decreased dispersion of these structures along peripheral microtubules.

Vesicle and organelle transport along microtubules can be both plus-end kinesin-directed and minus-end dynein-directed. We demonstrated that most remnant peroxisomes of PEX1-null and D-BP-deficient cells were still aligned with microtubules, but principally with the more centrally located regions of microtubules. Clustering of these structures was also observed in many cells, but this was not specifically at the MTOC – this effect therefore does not appear to represent a shift to minus-end transport. Instead, the general defect is more consistent with an inability of remnant peroxisomes, once associated with centrally located segments of microtubules, to travel towards the cell periphery. Our additional data indicate that microtubule morphology and function per se are not affected in these cells, but that the loss of microtubule-mediated plus-end peroxisome dispersal is inherent in the molecular properties of the abnormal peroxisomal structures.

A possible explanation for the observed clustering of remnant peroxisomes, is that they are sequestered for pexophagy (Farre and Subramani, 2004). However several lines of evidence do not support this view. First, peroxisomal ghosts did not colocalize with lysosomes, in agreement with previous findings (Santos et al., 2000). Second, most remnant peroxisomes still aligned with microtubules, implying residual biological function. Finally, PEX11β overexpression restored the abundance and distribution of remnant peroxisomes along peripheral microtubules, indicating that these structures are proliferation- and transport-competent.

The effect of PEX11βmyc overexpression is of particular significance in considering a molecular basis for these changes. The earlier findings of Gould and co-workers demonstrated that elevated levels of PEX11βmyc lead to increased peroxisome abundance (Chang et al., 1999; Li and Gould, 2002). Our data extend these findings in demonstrating that PEX11β restores the distribution of newly formed peroxisomal structures along peripheral microtubules. Thus, microtubule-mediated distribution of the peroxisomal structures in these cells is dependent on the abundance of peroxisomes: overexpression of PEX11β, in inducing peroxisome proliferation, also drives the plus-end dispersal of the newly synthesized organelles.

The other feature common to the peroxisomal structures of fibroblasts from ZS and D-BP-deficient patients is their increased size. ZS cells contain enlarged peroxisomal ghosts (Santos et al., 2000; Santos et al., 1988), whereas the enlarged
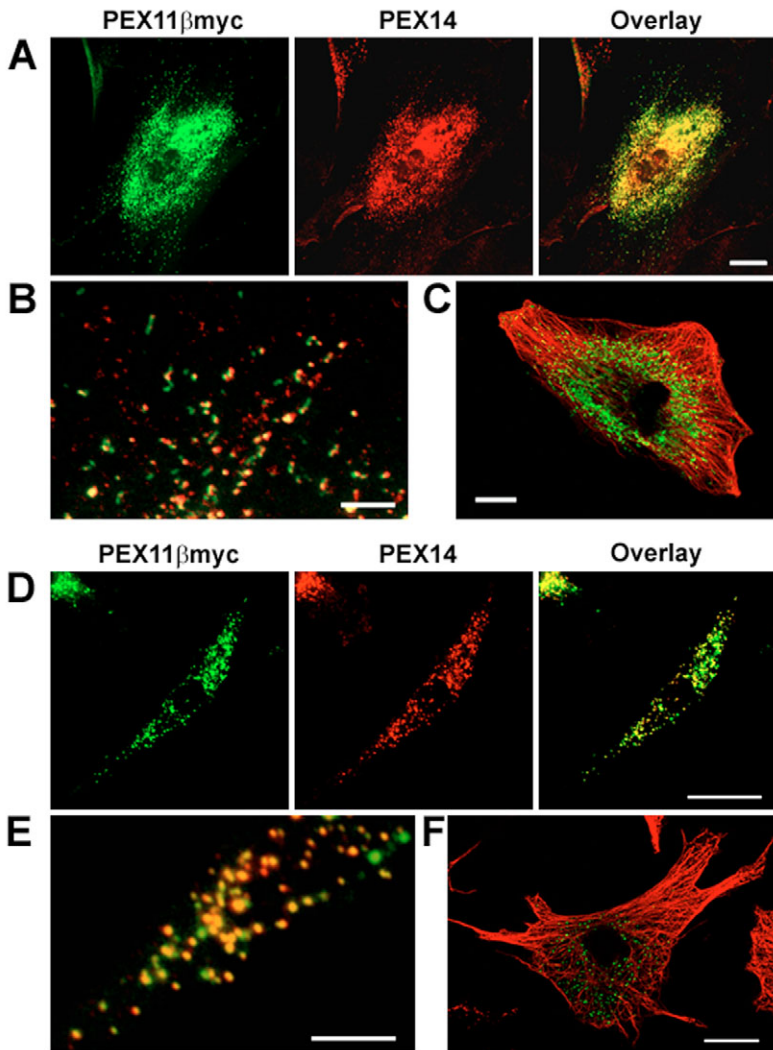


**Fig. 7.** PEX11β-myc overexpression leads to remnant peroxisome proliferation and redistribution along microtubules in PEX1-null and D-BP deficient cells. (A-C) PEX1-null and (D-F) D-BP-deficient patient HSFs stably expressing human PEX11βmyc. For epifluorescence microscopy, cells were double-labeled with PEX14 antibody (red) and myc antibody (green) (A,B,D,E). Panels B and E are magnifications of regions shown in overlay panels in A and D, respectively. For confocal laser-scanning microscopy, cells were double-labeled with PEX14 antibody (green) and α-tubulin antibody (red) (C and F). Bars, 20 μm (A,C,D,F); 5 μm (B,E).
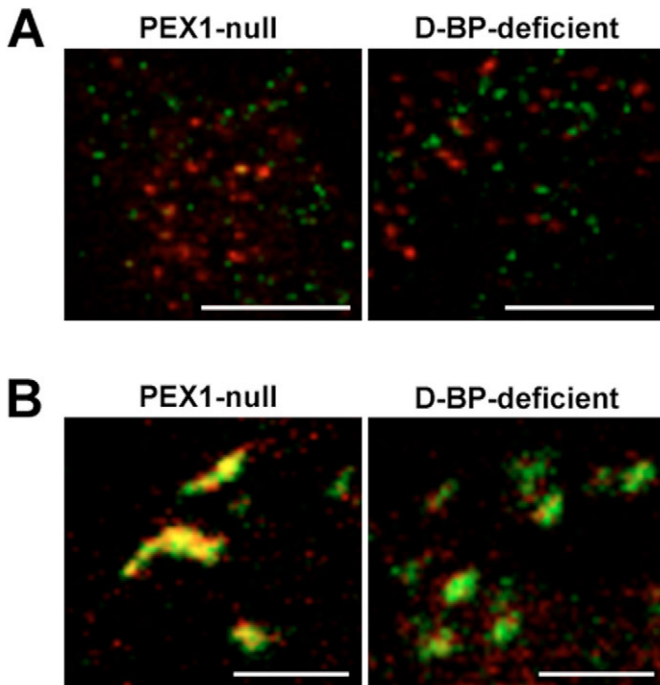
peroxisomes in D-BP-deficient cells presumably selectively lack D-BP. Given the known effect of PEX11β in inducing peroxisome proliferation, it is conceivable that these enlarged structures represent intermediates blocked in the process of peroxisome formation. In the main pathway of peroxisome biogenesis, new peroxisomes form from pre-existing peroxisomes through a pathway of elongation and division (Gould and Valle, 2000; Lazarow and Fujiki, 1985; Purdue and Lazarow, 2001). Although the exact function of PEX11β is unclear, it has been shown to induce peroxisome proliferation in normal cells – peroxisomes are converted from spherical-shaped organelles into elongated tubules and then back into spherical structures (Schrader et al., 1998). An essential role for PEX11β in peroxisome formation is also indicated by the finding that peroxisomes in hepatocytes from PEX11β-null mice are less abundant, clustered and elongated (Li et al., 2002b; Li and Gould, 2002). It is therefore possible that peroxisomal structures in ZS and D-BP-deficient cells have initiated expansion (reflected in enlarged structures) but not progressed to division. Surprisingly, however, we found remarkably different responses of these cells to overexpression of PEX11β. In D-BP-deficient cells, induced peroxisomes had the same spherical morphology as the parent peroxisomes, implying that peroxisome division was driven to completion. By contrast, in PEX1-null cells, induced peroxisomes displayed elongated, tubular structures displaying a PEX11βmyc banding pattern. These structures appear

identical to those described at early stages following transfection of normal human skin fibroblasts with PEX11β, which were interpreted to reflect membrane sub-domains where PEX11β segregates prior to the division step (Schrader et al., 1998). It therefore appears that PEX11βmyc overexpression in PEX1-null cells induces elongation and tubulation of the peroxisomal ghosts, but is not sufficient to efficiently drive the division step. Thus the peroxisomal structures in PEX1-null cells and D-BP deficient cells are similar in being stalled at the proliferation process, but differ in their capacity to be driven through the division step.

What molecular changes could explain the reduced peroxisome abundance and the different response to PEX11β overexpression? One protein implicated in the PEX11β-mediated process of peroxisome division is DLP1, a large dynamin-like GTPase protein (Yoon et al., 1998) that tubulates vesicle membranes in a nucleotide-dependent manner (Yoon et al., 2001). DLP1 is necessary only for the fission step of peroxisome division (Koch et al., 2004; Koch et al., 2003; Li and Gould, 2003) and is recruited to the peroxisomal membrane by PEX11β (Li and Gould, 2003). Significantly, disruption of DLP1 function reduces peroxisome abundance and generates organelles with long, tubular morphology (Koch et al., 2004; Koch et al., 2003; Li and Gould, 2003). The structures and peroxisome profile reported in these studies are similar to those we observed in PEX1-null cells overexpressing PEX11β-myc. Thus, reduced peroxisome abundance and the generation of tubular peroxisomes following a PEX11β-proliferative challenge are features compatible with those resulting from abrogation of cellular DLP1 function. In evaluating this link, we established that, as expected, DLP1 was absent from the majority of peroxisomal structures in (untransfected) D-BP deficient cells and PEX1-null cells. In cells overexpressing PEX11β-myc, however, DLP1 was found on membranes of some peroxisomes of D-BP-deficient cells, and at apparent higher levels on membranes of the elongated, tubular structures induced in PEX1-null cells. In the case of PEX1-null cells, the retention of DLP1 on induced peroxisomal tubules suggests that PEX11β-myc has successfully recruited DLP1 to these membranes, but that the process of fission is blocked at a subsequent, currently unknown step.

In these investigations, we have focused on the role of PEX11β in peroxisome proliferation because of its established role in peroxisome proliferation and its known involvement in recruiting DLP1 to the peroxisomal membrane. However, the PEX11 family also includes PEX11α and PEX11γ. Although these proteins are not apparently associated with significant changes to peroxisome abundance, PEX11γ at least may have some role in peroxisome tubulation, enlargement and clustering (Li et al., 2002a). Therefore, future experiments focusing on the levels of these two PEX11 proteins in patient cells may be warranted.

As to the role of microtubules in these processes, we propose that peroxisome proliferation and division on one hand, and peroxisome binding to microtubules on the other hand, are mechanistically linked processes. It is possible that peroxisome proliferation triggers the binding and transport of newly formed peroxisomes along microtubules. Indeed, it has been suggested that peroxisome division would require microtubule motor proteins to facilitate the constriction and subsequent



**Fig. 8.** PEX11βmyc overexpression recruits DLP1 to peroxisomal structures in PEX1-null and D-BP-deficient cells. (A) Confocal laser-scanning microscopy of untransfected PEX1-null fibroblasts, and fibroblasts from patients deficient in D-BP double-labeled with PEX14 antibody (red) and DLP1 antibody (green). (B) Confocal laser-scanning microscopy of PEX1-null and D-BP-deficient cells stably expressing PEX11βmyc, and double labeled with c-myc antibody (green) and DLP1 antibody (red). Bars, 20 μm (A); 5 μm (B).

division of peroxisomes (Koch et al., 2003). This is in accord with recent findings that demonstrate a requirement for microtubules in the earliest stages of peroxisome biogenesis (Brocard et al., 2005).

What is the potential impact of defective microtubule-mediated peroxisome transport? In normal cells, peroxisome transport to cytoplasmic regions would be necessary for specific metabolic imperatives, such as oxidation of fatty acids, synthesis of ether lipids, or disposal of reactive oxygen species. Interestingly, one of the common pathological consequences of ZS, D-BP deficiency and acyl-CoA oxidase deficiency, is neurodegeneration. In this investigation, we established that cultured brain neurons from the PEX13-null mouse also exhibit a reduction in abundance, and loss of distribution, of remnant peroxisomes along peripheral microtubules. We therefore speculate that loss of peroxisome trafficking in typical high-energy-dependent, multi-polar brain neurons could lead to degeneration of these cells. Equally, regional loss of peroxisomes could lead to oxidative damage. Indeed, overexpression of tau, which inhibits kinesin-dependent transport of peroxisomes, increases vulnerability of neurons to oxidative stress (Stamer et al., 2002). Regional loss of essential peroxisomal metabolism would also appear to reconcile the ZS-like phenotype of the PEX11β-null mouse, characterized by reduced peroxisome abundance, peroxisome clustering, and a mild defect in neuronal migration (Li et al., 2002b). However it remains to be established whether regional loss of peroxisomal activities are causative in the molecular pathogenesis of these disorders.

## Materials and Methods
### Plasmid constructs
A pcDNA3-based plasmid encoding human PEX11β protein fused to a C-terminal myc epitope tag (pcDNA3-PEX11β) was created by PCR of human cDNA using primers PEX11β-F 5′-GGTGGTGTTGGATCCGTCATGGACGCCTGGGTCC-GCTTCAGTG-3′ and PEX11β-myc-R 5′-GGTGTTGAATTCTCACAGGTCC-TCCTCGGAGATCAGCTTCTGCTCGGGCTTGAGTCGTAGCCAGGGATAG-3′ (myc tag codons underlined). The product was cloned into the *Bam*HI/*Eco*RI sites of pcDNA3 (Gibco-Invitrogen, Melbourne, Australia). The PTS2-EGFP plasmid, encoding the minimal rat PTS2 signal fused to the N-terminal end of EGFP, has been described (Maxwell et al., 2003). A pcDNA3-based plasmid expressing PTS1 fused to the C-terminus of EGFP was a gift from S. Gould (Johns Hopkins University, Baltimore, MD). The mouse PEX14 ORF was isolated by PCR from brain cDNA of C57BL/6J wild-type mice using the primers JB303 5′-CCCAAGCTTATGGCGTCGCTCGGAGCAGGCAGGAG-3′ (restriction enzyme site underlined) and JB304 5′-CGCGGATCCCTAGTCTCGCTCAGTCTCATTGC-TGG-3′. This product was cloned into the *Hind*III/*Bam*HI sites of pcDNA3 (Gibco-Invitrogen) to generate pcDNA3-MmPEX14. To generate an expression plasmid encoding a maltose-binding protein (MBP) fusion with full-length mouse PEX14 protein (MBP-MmPEX14), a PCR product obtained using pcDNA3-MmPEX14 template and primers JB305 5′-CTAGTCTAGAATGGCGTCGCTCGGAGCAGG-CAGAG-3′ and JB307 5′-AAAACTGCAGCTAGTCTCGCTCAGTCTCATTGC-TGG-3′, was cloned into the *Xba*I/*Pst*I sites of pMal-c2 (New England Biolabs, Beverly, MA). A second expression plasmid, encoding a glutathione-S-transferase (GST) fusion with full-length PEX14 (GST-MmPEX14), was generated by PCR from the same template using primers JB308 5′-ACGCGTCGACATGGCG-TCGTCGGAGCAGGCAGAG-3′ and JB310 5′-ATAAGAATGCGGCCGCGTC-TCGCTCAGTCTCATTGCTGG-3′, and cloned into the *Sal*I/*Not*I sites of pGEX5x-3 (Amersham plc, Buckinghamshire, UK). The fusion proteins were expressed in bacteria and purified using protocols previously described (Bjorkman et al., 2002; Crane et al., 1994; Gould et al., 1996; Urquhart et al., 2000).

### Cells and cell culture
Human skin fibroblasts (HSFs) from a PEX1-null ZS patient (4065) and an infantile Refsum disease (IRD) patient with residual PEX1 activity (1772) have been previously characterized (Maxwell et al., 2002). The D-BP deficient (patient IC) (Paton and Pollard, 2000; Paton et al., 1996), X-ALD and PEX7-deficient RCDP cell lines were from patients with typical clinical and biochemical findings for the respective disorder. In each case, diagnosis was confirmed by molecular analysis of the relevant gene. Mouse embryonic fibroblast (MEF) cultures were generated from day 13 p.c. embryos. Embryos were extracted, minced and incubated in 0.25%

trypsin in Earle's balanced salt solution overnight at 4°C (Freshney, 1994), the tissue triturated, and cellular debris allowed to settle under gravity. The supernatant containing dispersed cells was removed and centrifuged at 250 *g* for 5 minutes and the cell pellets resuspended in culture medium. All fibroblasts were cultured in Dulbecco's modified Eagle's medium: Ham F12 supplemented with 10% fetal bovine serum (FBS), 2 mM L-glutamine, and 100 μg/ml penicillin, 100 U/ml streptomycin (Gibco-Invitrogen). Cells were trypsinized and seeded onto coverslips at a density to achieve approx. 60-70% confluency 16-20 hours later, then processed for immunofluorescence. PEX1-null and D-BP deficient skin fibroblast cell lines stably expressing PEX11β were obtained by transfection with 8 μg pcDNA3-PEX11βmyc (or pcDNA3, mock transfection) using the Lipofectamine 2000 transfection reagent (Gibco-Invitrogen), followed by selection using 400 μM Geneticin (Gibco-Invitrogen). The microtubule network of cells grown on glass coverslips was dispersed by addition of 20 μM nocodazole (Sigma, St Louis, MO) to the culture medium for 20 hours prior to fixation. Mouse neuronal cell cultures were established from whole brain tissue samples treated overnight at 4°C with 1 ml of 0.25% trypsin in cold Earle's balanced salt solution (Gibco-Invitrogen). Digested tissue was incubated at 37°C for 20 minutes, after which 4 ml DMEM-F12 containing 10% fetal bovine serum, L-glutamine and penicillin/streptomycin was added. Dissociated cells were resuspended in Neurobasal-A medium (Gibco-Invitrogen) containing B27 supplement and 10 μg/ml NGF (Gibco-Invitrogen), and seeded onto coverslips coated with poly-L-lysine. Ethics approval for the use of human skin fibroblasts was obtained from both the Adelaide Women's and Children's Hospital Research Ethics Committee and the Griffith University Human Ethics Committee, and for animal use from the Griffith University Animal Ethics Committee.

### Antibodies and fluorescence microscopy
PEX14 polyclonal antibodies raised against MBP-MmPEX14 fusion protein were purified from rabbit serum by affinity chromatography using GST-MmPEX14 fusion protein covalently coupled to CNBr-activated Sepharose. Mouse monoclonal antibodies to human α-tubulin were from Sigma-Aldrich (St Louis, MO) and to human DLP1 from BD Biosciences (Palo Alto, CA). Goat anti-mouse Alexa Fluor 488 and 568, and goat anti-rabbit Alexa Fluor 488 and 568 secondary antibodies, were obtained from Molecular Probes (Eugene, OR). Chicken c-myc antibody and FITC-conjugated goat anti-chicken IgG were from Santa Cruz Biotechnology (Santa Cruz, CA). Indirect immunofluorescence was carried out as previously described (Maxwell et al., 2003; Maxwell et al., 2002) for human skin fibroblasts permeabilized with either 1% Triton X-100) or 25 μg/ml digitonin. Epifluorescence microscopy was carried out using a Nikon Eclipse E600 fluorescence microscope, with image acquisition using a Photometrics Coolsnap digital camera (Roper Scientific) and V++ Imaging software. Confocal laser-scanning microscopy was carried out using a Leica TCS SP2 microscope (Leica Microsystems Heidelberg, Germany). Quantification of peroxisomal abundance and size was carried out using a MAT-lab-based algorithm (Pham et al., 2004) and expressed as the mean ± s.e.m. of five or more separate cell analyses, from experiments replicated at least twice. Mitochondria were visualized by fluorescence microscopy following incubation of cultured cells for 45 minutes in medium containing 400 nM MitoTracker Red CM-H$_2$XRos or MitoTracker Green FM (Molecular Probes, Eugene, OR). Lysosomes were similarly visualized following incubation of cells for 2 hours in medium containing 100 nM LysoTracker Red DND-99 (Molecular Probes, Eugene, OR). Identification of neurons and astrocytes in cultures was based on morphological criteria and fluorescence microscopy using antibodies to the cell-specific markers neurofilament 200 (Sigma) and GFAP (DAKO, Carpinteria, Denmark), respectively.

### Liver fractionation and western blot analysis
Differential centrifugation of mouse liver homogenates to generate a large organelle fraction (containing peroxisomes, mitochondria, and lysosomes) and a post-organellar supernatant, and western blot analysis of these fractions, was carried out as previously described (Maxwell et al., 2003).

## References
**Aridor, M. and Hannan, L. A.** (2000). Traffic jam: a compendium of human diseases that affect intracellular transport processes. *Traffic* **1**, 836-851.
**Bjorkman, J., Gould, S. J. and Crane, D. I.** (2002). Pex13, the mouse ortholog of the

human peroxisome biogenesis disorder PEX13 gene: gene structure, tissue expression, and localization of the protein to peroxisomes. *Genomics* **79**, 162-168.

**Brocard, C. B., Boucher, K. K., Jedeszko, C., Kim, P. K. and Walton, P. A.** (2005). Requirement for microtubules and Dynein motors in the earliest stages of peroxisome biogenesis. *Traffic* **6**, 386-395.

**Chang, C. C., South, S., Warren, D., Jones, J., Moser, A. B., Moser, H. W. and Gould, S. J.** (1999). Metabolic control of peroxisome abundance. *J. Cell Sci.* **112**, 1579-1590.

**Crane, D. I., Kalish, J. E. and Gould, S. J.** (1994). The Pichia pastoris PAS4 gene encodes a ubiquitin-conjugating enzyme required for peroxisome assembly. *J. Biol. Chem.* **269**, 21835-21844.

**Farre, J. C. and Subramani, S.** (2004). Peroxisome turnover by micropexophagy: an autophagy-related process. *Trends Cell Biol.* **14**, 515-523.

**Fransen, M., Terlecky, S. R. and Subramani, S.** (1998). Identification of a human PTS1 receptor docking protein directly required for peroxisomal protein import. *Proc. Natl. Acad. Sci. USA* **95**, 8087-8092.

**Freshney, R. I.** (1994). *Culture of Animal Cells: A Manual of Basic Techniques*. New York: Wiley-Liss.

**Gould, S. J. and Valle, D.** (2000). Peroxisome biogenesis disorders: genetics and cell biology. *Trends Genet.* **16**, 340-345.

**Gould, S. J., Kalish, J. E., Morrell, J. C., Bjorkman, J., Urquhart, A. J. and Crane, D. I.** (1996). Pex13p is an SH3 protein of the peroxisome membrane and a docking factor for the predominantly cytoplasmic PTs1 receptor. *J. Cell Biol.* **135**, 85-95.

**Gould, S. J., Valle, D. and Raymond, G. V.** (2001). The peroxisome biogenesis disorders. In *The Metabolic and Molecular Bases of Inherited Disease*, vol. 2 (eds. C. R. Scriver, A. L. Beaudet, W. S. Sly and D. Valle), pp. 3181-3217. New York: McGraw-Hill.

**Hughes, J. L., Poulos, A., Robertson, E., Chow, C. W., Sheffield, L. J., Christodoulou, J. and Carter, R. F.** (1990). Pathology of hepatic peroxisomes and mitochondria in patients with peroxisomal disorders. *Virchows Arch. A Pathol. Anat. Histopathol.* **416**, 255-264.

**Koch, A., Thiemann, M., Grabenbauer, M., Yoon, Y., McNiven, M. A. and Schrader, M.** (2003). Dynamin-like protein 1 is involved in peroxisomal fission. *J. Biol. Chem.* **278**, 8597-8605.

**Koch, A., Schneider, G., Luers, G. H. and Schrader, M.** (2004). Peroxisome elongation and constriction but not fission can occur independently of dynamin-like protein 1. *J. Cell Sci.* **117**, 3995-4006.

**Lazarow, P. B. and Fujiki, Y.** (1985). Biogenesis of peroxisomes. *Annu. Rev. Cell Biol.* **1**, 489-530.

**Li, X. and Gould, S. J.** (2002). PEX11 promotes peroxisome division independently of peroxisome metabolism. *J. Cell Biol.* **156**, 643-651.

**Li, X. and Gould, S. J.** (2003). The dynamin-like GTPase DLP1 is essential for peroxisome division and is recruited to peroxisomes in part by PEX11. *J. Biol. Chem.* **278**, 17012-17020.

**Li, X., Baumgart, E., Dong, G. X., Morrell, J. C., Jimenez-Sanchez, G., Valle, D., Smith, K. D. and Gould, S. J.** (2002a). PEX11alpha is required for peroxisome proliferation in response to 4-phenylbutyrate but is dispensable for peroxisome proliferator-activated receptor alpha-mediated peroxisome proliferation. *Mol. Cell. Biol.* **22**, 8226-8240.

**Li, X., Baumgart, E., Morrell, J. C., Jimenez-Sanchez, G., Valle, D. and Gould, S. J.** (2002b). PEX11 beta deficiency is lethal and impairs neuronal migration but does not abrogate peroxisome function. *Mol. Cell. Biol.* **22**, 4358-4365.

**Maxwell, M. A., Nelson, P. V., Chin, S. J., Paton, B. C., Carey, W. F. and Crane, D. I.** (1999). A common PEX1 frameshift mutation in patients with disorders of peroxisome biogenesis correlates with the severe Zellweger syndrome phenotype. *Hum. Genet.* **105**, 38-44.

**Maxwell, M. A., Allen, T., Solly, P. B., Svingen, T., Paton, B. C. and Crane, D. I.** (2002). Novel PEX1 mutations and genotype-phenotype correlations in Australasian peroxisome biogenesis disorder patients. *Hum. Mutat.* **20**, 342-351.

**Maxwell, M., Bjorkman, J., Nguyen, T., Sharp, P., Finnie, J., Paterson, C., Tonks, I., Paton, B. C., Kay, G. F. and Crane, D. I.** (2003). Pex13 inactivation in the mouse disrupts peroxisome biogenesis and leads to a Zellweger syndrome phenotype. *Mol. Cell. Biol.* **23**, 5947-5957.

**Moser, H. W.** (1993). Peroxisomal diseases. *Adv. Hum. Genet.* **21**, 1-106, 443-451.

**Moser, H. W.** (1996). Peroxisomal disorders. *Semin. Pediatr. Neurol.* **3**, 298-304.

**Paton, B. C. and Pollard, A. N.** (2000). Molecular changes in the D-bifunctional protein cDNA sequence in Australasian patients belonging to the bifunctional protein complementation group. *Cell Biochem. Biophys.* **32**, 247-251.

**Paton, B. C., Sharp, P. C., Crane, D. I. and Poulos, A.** (1996). Oxidation of pristanic acid in fibroblasts and its application to the diagnosis of peroxisomal beta-oxidation defects. *J. Clin. Invest.* **97**, 681-688.

**Pham, T. D., Crane, D. I., Tran, T. H. and Nguyen, T. H.** (2004). Extraction of fluorescent cell puncta by adaptive fuzzy segmentation. *Bioinformatics* **20**, 2189-2196.

**Poll-The, B. T., Roels, F., Ogier, H., Scotto, J., Vamecq, J., Schutgens, R. B., Wanders, R. J., van Roermund, C. W., van Wijland, M. J., Schram, A. W. et al.** (1988). A new peroxisomal disorder with enlarged peroxisomes and a specific deficiency of acyl-CoA oxidase (pseudo-neonatal adrenoleukodystrophy). *Am. J. Hum. Genet.* **42**, 422-434.

**Purdue, P. E. and Lazarow, P. B.** (2001). Peroxisome biogenesis. *Annu. Rev. Cell Dev. Biol.* **17**, 701-752.

**Purdue, P. E., Zhang, J. W., Skoneczny, M. and Lazarow, P. B.** (1997). Rhizomelic chondrodysplasia punctata is caused by deficiency of human PEX7, a homologue of the yeast PTS2 receptor. *Nat. Genet.* **15**, 381-384.

**Purdue, P. E., Skoneczny, M., Yang, X., Zhang, J. W. and Lazarow, P. B.** (1999). Rhizomelic chondrodysplasia punctata, a peroxisomal biogenesis disorder caused by defects in Pex7p, a peroxisomal protein import receptor: a minireview. *Neurochem. Res.* **24**, 581-586.

**Rapp, S., Saffrich, R., Anton, M., Jakle, U., Ansorge, W., Gorgas, K. and Just, W. W.** (1996). Microtubule-based peroxisome movement. *J. Cell Sci.* **109**, 837-849.

**Santos, M. J., Imanaka, T., Shio, H. and Lazarow, P. B.** (1988). Peroxisomal integral membrane proteins in control and Zellweger fibroblasts. *J. Biol. Chem.* **263**, 10502-10509.

**Santos, M. J., Henderson, S. C., Moser, A. B., Moser, H. W. and Lazarow, P. B.** (2000). Peroxisomal ghosts are intracellular structures distinct from lysosomal compartments in Zellweger syndrome: a confocal laser scanning microscopy study. *Biol. Cell* **92**, 85-94.

**Schrader, M.** (2001). Tubulo-reticular clusters of peroxisomes in living COS-7 cells: dynamic behavior and association with lipid droplets. *J. Histochem. Cytochem.* **49**, 1421-1429.

**Schrader, M., Burkhardt, J. K., Baumgart, E., Luers, G., Spring, H., Volkl, A. and Fahimi, H. D.** (1996). Interaction of microtubules with peroxisomes. Tubular and spherical peroxisomes in HepG2 cells and their alterations induced by microtubule-active drugs. *Eur. J. Cell Biol.* **69**, 24-35.

**Schrader, M., Reuber, B. E., Morrell, J. C., Jimenez-Sanchez, G., Obie, C., Stroh, T. A., Valle, D., Schroer, T. A. and Gould, S. J.** (1998). Expression of PEX11beta mediates peroxisome proliferation in the absence of extracellular stimuli. *J. Biol. Chem.* **273**, 29607-29614.

**Schrader, M., King, S. J., Stroh, T. A. and Schroer, T. A.** (2000). Real time imaging reveals a peroxisomal reticulum in living cells. *J. Cell Sci.* **113**, 3663-3671.

**Schrader, M., Thiemann, M. and Fahimi, H. D.** (2003). Peroxisomal motility and interaction with microtubules. *Microsc. Res. Tech.* **61**, 171-178.

**Schutgens, R. B. H., Heymans, H. S. A., Wanders, R. J. A., van den Bosch, H. and Tager, J. M.** (1986). Peroxisomal disorders: a newly recognized group of genetic diseases. *Eur. J. Pediatr.* **144**, 430-440.

**Shimizu, N., Itoh, R., Hirono, Y., Otera, H., Ghaedi, K., Tateishi, K., Tamura, S., Okumoto, K., Harano, T., Mukai, S. et al.** (1999). The peroxin Pex14p. cDNA cloning by functional complementation on a Chinese hamster ovary cell mutant, characterization, and functional analysis. *J. Biol. Chem.* **274**, 12593-12604.

**Smith, K. D., Kemp, S., Braiterman, L. T., Lu, J. F., Wei, H. M., Geraghty, M., Stetten, G., Bergin, J. S., Pevsner, J. and Watkins, P. A.** (1999). X-linked adrenoleukodystrophy: genes, mutations, and phenotypes. *Neurochem. Res.* **24**, 521-535.

**Stamer, K., Vogel, R., Thies, E., Mandelkow, E. and Mandelkow, E. M.** (2002). Tau blocks traffic of organelles, neurofilaments, and APP vesicles in neurons and enhances oxidative stress. *J. Cell Biol.* **156**, 1051-1063.

**Suzuki, Y., Shimozawa, N., Yajima, S., Tomatsu, S., Kondo, N., Nakada, Y., Akaboshi, S., Lai, M., Tanabe, Y., Hashimoto, T. et al.** (1994). Novel subtype of peroxisomal acyl-CoA oxidase deficiency and bifunctional enzyme deficiency with detectable enzyme protein: identification by means of complementation analysis. *Am. J. Hum. Genet.* **54**, 36-43.

**Thiemann, M., Schrader, M., Volkl, A., Baumgart, E. and Fahimi, H. D.** (2000). Interaction of peroxisomes with microtubules. In vitro studies using a novel peroxisome-microtubule binding assay. *Eur. J. Biochem.* **267**, 6264-6275.

**Urquhart, A. J., Kennedy, D., Gould, S. J. and Crane, D. I.** (2000). Interaction of Pex5p, the type 1 peroxisome targeting signal receptor, with the peroxisomal membrane proteins Pex14p and Pex13p. *J. Biol. Chem.* **275**, 4127-4136.

**van den Bosch, H., Schutgens, R. B. H., Wanders, R. J. A. and Tager, J. M.** (1992). Biochemistry of peroxisomes. *Annu. Rev. Biochem.* **61**, 157-197.

**van Grunsven, E. G., van Berkel, E., Mooijer, P. A., Watkins, P. A., Moser, H. W., Suzuki, Y., Jiang, L. L., Hashimoto, T., Hoefler, G., Adamski, J. et al.** (1999). Peroxisomal bifunctional protein deficiency revisited: resolution of its true enzymatic and molecular basis. *Am. J. Hum. Genet.* **64**, 99-107.

**Wanders, R. J. and Waterham, H. R.** (2005). Peroxisomal disorders I: biochemistry and genetics of peroxisome biogenesis disorders. *Clin. Genet.* **67**, 107-133.

**Wanders, R. J., Schutgens, R. B. and Barth, P. G.** (1995). Peroxisomal disorders: a review. *J. Neuropathol. Exp. Neurol.* **54**, 726-739.

**Weller, S., Gould, S. J. and Valle, D.** (2003). Peroxisome biogenesis disorders. *Annu. Rev. Genomics Hum. Genet.* **4**, 165-211.

**Welte, M. A.** (2004). Bidirectional transport along microtubules. *Curr. Biol.* **14**, R525-R537.

**Wiemer, E. A., Wenzel, T., Deerinck, T. J., Ellisman, M. H. and Subramani, S.** (1997). Visualization of the peroxisomal compartment in living mammalian cells: dynamic behavior and association with microtubules. *J. Cell Biol.* **136**, 71-80.

**Yoon, Y., Pitts, K. R., Dahan, S. and McNiven, M. A.** (1998). A novel dynamin-like protein associates with cytoplasmic vesicles and tubules of the endoplasmic reticulum in mammalian cells. *J. Cell Biol.* **140**, 779-793.

**Yoon, Y., Pitts, K. R. and McNiven, M. A.** (2001). Mammalian dynamin-like protein DLP1 tubulates membranes. *Mol. Biol. Cell* **12**, 2894-2905.